RSC Advances

ROYAL SOCIETY OF CHEMISTRY

www.rsc.org/advances

Eu^{2+}-Activated Full Color Orthophosphate Phosphors for Warm White Light-Emitting Diodes

Chenglong Zhao[a], Zhiguo Xia[a,b,*], Molin Li[a]

[a]*School of Materials Sciences and Technology, China University of Geosciences, Beijing 100083, China*

[b]*School of Materials Sciences and Engineering, University of Science and Technology Beijing, Beijing 100083, China*

Eu^{2+}-activated full color versatile orthophosphate phosphors can find potential application in warm white LEDs.

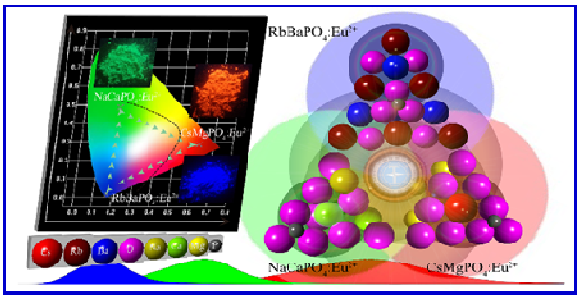

Eu^{2+}-Activated Full Color Orthophosphate Phosphors for Warm White Light-Emitting Diodes

Chenglong Zhao[a], Zhiguo Xia[a,b,*], Molin Li[a]

[a]*School of Materials Sciences and Technology, China University of Geosciences, Beijing 100083, China*

[b]*School of Materials Sciences and Engineering, University of Science and Technology Beijing, Beijing 100083, China*

---

[*]Author to whom correspondence should be addressed: **Zhiguo Xia,**

e-mail: xiazg@ustb.edu.cn

Tel. : +86-10-8237-7955;

Fax. : +86-10-8237-7955

Address: School of Materials Sciences and Engineering, University of Science and Technology Beijing, Beijing 100083, China

---

Abstract:

Eu^{2+}-doped $RbBaPO_4$, $NaCaPO_4$ and $CsMgPO_4$ orthophosphate phosphors were studied in this paper. X-ray diffraction patterns (XRD) analysis indicated all of the phosphors could be obtained in pure phase by the solid-state reaction method. The photoluminescence emission (PL) spectra exhibited that the phosphors showed broad-band blue, green and red emission with peaks at near 430 nm, 510 nm and 630 nm under 340 nm UV lamp, corresponding to $RbBaPO_4$:0.03Eu^{2+}, $NaCaPO_4$:0.01Eu^{2+} and $CsMgPO_4$:0.07Eu^{2+} samples, respectively. A white-light-emitting diodes (*w*-LEDs) lamp fabricated by the three samples combining a 370 nm n-UV chip presented a high color rendering indices (CRI) of 86 as well as a warm correlated color temperatures (CCT) of 2751K. The results indicated that Eu^{2+}-activated full color versatile orthophosphate phosphors and mixing strategy of the similar hosts will be potential for the design of the white LEDs.

Ⅰ. Introduction

Since the first white-light-emitting diodes (*w*-LEDs) were commercially available in 1997, it had drawn a lot of attentions for advantages of high luminous efficiency, energy savings and low power consumption and so on[1-2]. The general way to fabricate white LEDs is based on a blue InGaN LED chip and a yellow phosphor YAG:Ce^{3+}, which perform poor color rendering index[3]. In order to improve the color rendering index (CRI), the ultraviolet/near-ultraviolet (UV/NUV) chip pumped of a phosphor blend of blue, green and red emission phosphors has been widely investigated recently[4]. The commercialized blue, green and red phosphors for white LED lamps, such as $BaMgAl_{10}O_{17}:Eu^{2+}$ (BAM), $Ba_2SiO_4:Eu^{2+}$ (BSO), $CaAlSiN_3:Eu^{2+}$ (CASN) and so on, have been used generally, but there exists a disadvantage that the different host families may lead to bad consistency in usage. In this work, we have synthesized three kinds of full color orthophosphate phosphors with a single rare-earth activator Eu^{2+} to explore the luminescent properties for white-light-emitting diodes (*w*-LEDs) application. Therefore, the same orthophosphate host family, including blue emission $RbBaPO_4:0.03Eu^{2+}$, green emission $NaCaPO_4:0.01Eu^{2+}$ and red emission $CsMgPO_4:0.07Eu^{2+}$ phosphors[5-7] are selected as tricolor emission for NUV LEDs to improve consistency for the application of white LED lamps[8].

II. Experimental Procedure

$RbBaPO_4:0.03Eu^{2+}$, $NaCaPO_4:0.01Eu^{2+}$ and $CsMgPO_4:0.07Eu^{2+}$phosphors were prepared via a traditional high temperature solid-state method. The stoichiometric

amounts of Rb_2CO_3 (A.R.), Na_2CO_3 (A.R.), Cs_2CO_3 (A.R.), $BaCO_3$ (A.R.), $CaCO_3$ (A.R.), $(MgCO_3)_4 \cdot Mg(OH)_2 \cdot 5H_2O$ (A.R.), $(NH_4)_2HPO_4$ (A.R.) and Eu_2O_3 (99.99%) were employed as the raw materials, which were mixed and ground homogeneously in the agate mortar. The mixture was firstly pre-heated at 500 ^oC for 3h in air atmosphere in alumina crucibles with covers. After the preliminary products were ground thoroughly in an agate mortar after cooling to room temperature, they were placed into alumina crucibles and annealed at 1150 °C in a CO reducing atmosphere for 3 h with highly pure carbon particles as a reducing agent. Then the phosphors were finally obtained for characterization.

Powder X-ray diffraction (XRD) data was checked for structural phase identification by an X-ray powder diffractometer (SHIMADZU, XRD-6000, Cu Kα radiation, λ = 0.15406 nm, 40 kV, 40 mA). The continuous scanning rate (2θ ranging from 5° to 90°) used as phase formation determination was 4^o(2θ)/min and step scanning rate (2θ ranging from 10° to 80°) used for Rietveld analysis was 8s/step with a step size of 0.02. Powder diffraction data were obtained using a computer software General Structure Analysis System (GSAS) program. The morphology of the samples were inspected using a scanning electron microscope (SEM, JEOL, JSM-6490). Room temperature photoluminescence excitation (PLE) and emission (PL) spectra were characterized on F-4600 fluorescence spectrophotometer (F-4600, HITACHI, Japan) with a photomultiplier tube operating at 400 V, and a 150 W Xe lamp used as the excitation source, the temperature-dependence luminescence properties were measured on the same spectrophotometer combined with a self-made heating attachment and a computer-controlled electric furnace. Optical properties of the

white-light *n*-UV LED including the luminescent spectrum, CRI, CCT, and CIE value of the lamp, were measured by a HAAS-2000 (Ever fine, China) light and radiation measuring instrument. The quantum efficiency (QE) was measured using the integrating sphere on the FLS920 fluorescence spectrophotometer (Edinburgh Instruments Ltd., UK), and a Xe900 lamp was used as an excitation source and white $BaSO_4$ powder as a reference.

III. Results and Discussion

(1) Phase structure

Fig. 1 shows the typical powder XRD patterns of $RbBaPO_4$:0.03Eu^{2+}, $NaCaPO_4$:0.01Eu^{2+} and $CsMgPO_4$:0.07Eu^{2+} samples and the standard datum reported in the Joint Committee on Powder Diffraction Standards card data (JCPDS-81-647-$RbBaPO_4$, JCPDS-39-1193-$NaCaPO_4$ and JCPDS-45-275-$CsMgPO_4$) given as the comparison[9-11]. We found that no impurity or significant changes were detected in the hosts, which confirmed these samples were successfully obtained by the solid-state reaction method. Furthermore, the refinements and data processing were performed by GSAS program[12] for further demonstrating their phase structures. As shown in Fig. 2 a), b) and c), there was not any impurities existing in the synthesized samples, and we also get the Rietveld results presented in Table 1, where we can see the volume of them are 448.86 $Å^3$, 1009.16 $Å^3$ and 474.49 $Å^3$, respectively, indicating the incorporation of Eu^{2+} in the host lattice. The reason is that, in the present work, ionic radii are $Ba^{2+}_{CN=9}$=1.47Å, $Ca^{2+}_{CN=7}$=1.06Å, $_{CN=8}$=1.12Å and $Cs^{+}_{CN=6}$=1.67Å, while the ionic radii for the six-, seven-, eight- and nine-coordinated Eu^{2+} are 1.17, 1.20, 1.25 and 1.30 Å[13], when doping small amount of Eu^{2+} to replace

the other ions will change the unit cell parameters and volume partly. What is more, we can see the values of R_{wp} and R_p are quite smaller, so the results can verify the phase formation.

(2) Luminescence properties

Photoluminescence excitation (PLE) and emission (PL) spectrum of $RbBaPO_4$:0.03Eu^{2+}, $NaCaPO_4$:0.01Eu^{2+} and $CsMgPO_4$:0.07Eu^{2+} phosphors are displayed in Fig. 3, where the concentration of Eu^{2+} in the three phosphors are all corresponds to the maximum of luminescence intensity from the previous reports respectively[5-7]. The excitation spectra are all composed of strong broad absorption bands from 200 to 420 nm UV and *n*-UV range attributed to $4f^7(^8S_{7/2})$-$4f^6 5d$ transitions of the doped Eu^{2+} ions[14]. Under the excitation at 340nm, the phosphors exhibited strong blue, green and red emission bands peaked at 430nm, 510nm and 630nm which can verify the possibility of the operation as the n-UV chip for *w*-LEDs application. In order to study the relationship between the coordination environment of Eu^{2+} and emission peaks, the following *Eq.*1 by Van Uitert were employed[15]:

$$E = Q\left[1-\left(\frac{V}{4}\right)^{\frac{1}{V}} 10^{-\frac{near}{80}}\right] \quad (1)$$

where E represents the position for the rare-earth ion emission peak (cm^{-1}), Q is the energy position of the lower *d*-band edge for the free ions (34,000 cm^{-1} for Eu^{2+}), V is the valence of the ‘‘active’’ cation (V = 2 for Eu^{2+}), n is the number of anions in the immediate shell around the ‘‘active’’ cation, r is the effective radius of the host cation replaced by the Eu^{2+} ion (Å), and ea is the electron affinity of the atoms that form anions (eV). The value of ea is the uncertainty in different circumstance, here, ea is about 1.60 or 2.19eV[15]. So by the semiquantitative calculation, we get the results of E are approximate to $Ba^{2+}{}_{CN=9}$=23558cm^{-1}, $Ca^{2+}{}_{CN=7}$=18939cm^{-1}, $_{CN=8}$=20333cm^{-1} and

$Cs^{+}_{CN=6}$=16325cm^{-1}, respectively. The Fig. 4 a) show the normalized emission spectra for $RbBaPO_4:Eu^{2+}$, $NaCaPO_4:Eu^{2+}$ and $CsMgPO_4:Eu^{2+}$ phosphors under the excitation at 340nm and Fig. 4 b) the coordination environment of the cations Ba^{2+}, Ca^{2+} and Cs^{+}, which illustrates Eu^{2+}-activated orthophosphate phosphors are assuredly able to realize the blue to red emission for white-light-emitting diodes (*w*-LEDs) application. In addition, a qualitative analysis about the relationship between crystal field splitting (ε_{cfs}) and coordination number or polyhedron size were discussed presented in Fig. 5. In this work, ε_c is the centroid shift measured from the excitation spectrum[16], $\varepsilon_c(RbBaPO_4:Eu^{2+}) < \varepsilon_c(NaCaPO_4:Eu^{2+}: Ca^{2+}_{CN=8}) < \varepsilon_c(NaCaPO_4:Eu^{2+}: Ca^{2+}_{CN=7}) < \varepsilon_c(CsMgPO_4:Eu^{2+})$. Dorenbos *et al*[17-19] have reported that the smaller the coordination number, the larger the crystal field splitting in various Ce^{3+}-doped phosphors. Similarly, the values of ε_{cfs} in Eu^{2+}-doped phosphors are $\varepsilon_{cfs}(RbBaPO_4:Eu^{2+}_{CN=9}) < \varepsilon_{cfs}(NaCaPO_4:Eu^{2+}_{CN=8}) < \varepsilon_{cfs}(NaCaPO_4:Eu^{2+}_{CN=7}) < \varepsilon_{cfs}(CsMgPO_4:Eu^{2+}_{CN=6})$. Therefore, we can get result that the larger ε_{cfs} and ε_c are, the smaller wavenumber is, which indicate $CsMgPO_4:Eu^{2+}$ shows up the longest emission wavelength at 630 nm among the above phosphors under the same excitation wavelength, and contributes much to the 5*d* crystal field splitting.

(3) Surface topography, thermal decay and quantum efficiency (QE) properties.

The surface topography of the $RbBaPO_4:Eu^{2+}$, $NaCaPO_4:Eu^{2+}$, $CsMgPO_4:Eu^{2+}$ and the mixture of those tri-color phosphors were inspected using a scanning electron microscope (SEM) to investigate the particle size. **Fig. 6** exhibit the SEM images of the a) $RbBaPO_4:Eu^{2+}$, b) $NaCaPO_4:Eu^{2+}$, c) $CsMgPO_4:Eu^{2+}$ and d) the mixture of those tri-color phosphors, respectively. It can be found that all the images are with a wide range of particle size including agglomerates of the smaller particles, but the particle size of a) $RbBaPO_4:Eu^{2+}$ compound are slightly bigger than the other two b)

$NaCaPO_4:Eu^{2+}$, c) $CsMgPO_4:Eu^{2+}$ compounds. However, when the three phosphors were mixed to acquire the w-LEDs lamp according to the ratio of 1:19:16 based on the relative intensity of emission spectrum from the same decay test conditions, the SEM image of the tri-color phosphors mixture was shown in **Fig. 6 d)**. **Fig. 6 d)** shows the particle size of the mixture was similar with those three individual samples. From the above results, it can be expected that $RbBaPO_4:Eu^{2+}$, $NaCaPO_4:Eu^{2+}$ and $CsMgPO_4:Eu^{2+}$ the three phosphors should be quite suitable to be fabricated for the potential application in white LEDs. The thermal decay and quantum efficiency (QE) properties have also measured. As shown in **Fig. 7**, the relative intensities of temperature-dependent emission spectra for $RbBaPO_4:Eu^{2+}$ and $NaCaPO_4:Eu^{2+}$ show the better thermal stabilities, but $CsMgPO_4:Eu^{2+}$ is inferior to the others under the excitation of 340 nm. The PL relative intensity $CsMgPO_4:Eu^{2+}$ at 423 K(150 ^{o}C) drops to 46.7% of the initial value at room temperature, and it seems to be a disadvantage to adopt this phosphor in the white LEDs application because of the low luminescence thermal stability. However, the other two phosphors all have better thermal stabilities, when the same orthophosphate phosphors of $RbBaPO_4:0.03Eu^{2+}$, $NaCaPO_4:0.01Eu^{2+}$ and $CsMgPO_4:0.07Eu^{2+}$ are in blending, the monolithic thermal stability should be improved for potential application in warm white LEDs. From the thermal stability results, it could be expected that the luminescence intensity of $CsMgPO_4:0.07Eu^{2+}$ would be with very low QE. Based on the following *Eq.*2[20],

$$\eta_{QE} = \int L_s / (\int E_R - \int E_s) \tag{2}$$

where L_S is the luminescence emission spectrum of the sample; E_S is the spectrum of the light used for exciting the sample; E_R is the spectrum of the excitation light without the sample in the sphere; and all the spectra were collected using the

integrating sphere. The measured internal QE values of $RbBaPO_4$:0.03Eu^{2+}, $NaCaPO_4$:0.01Eu^{2+} and $CsMgPO_4$:0.07Eu^{2+} phosphors are determined as about 54.06%, 36.33% and 13.40% under 340nm excitation, respectively. The QEs values are in accord with the results of thermal stability property.

(4) CIE chromaticity coordinates and electroluminescence properties.

The CIE chromaticity diagrams for $RbBaPO_4$:Eu^{2+}, $NaCaPO_4$:Eu^{2+} and $CsMgPO_4$:Eu^{2+} phosphors are displayed in Fig.8, and the insets show the digital phosphor photos under 365 nm UV-lamp excitation. All phosphors show intense emission, which indicates they can be applied to the white light-emitting diodes as the three primary color components. In order to evaluate the actual potential application of the phosphors for *pc*-WLEDs, a *w*-LED lamp was successfully fabricated by the combination of a 370 nm *n*-UV InGaN chip and blue emission $RbBaPO_4$:Eu^{2+}, green emission $NaCaPO_4$:Eu^{2+} as well as red emission $CsMgPO_4$:Eu^{2+} phosphors, the ratio of the content of three phosphors for the fabrication are 1:19:16 based on the relative intensity of emission spectrum from the same decay test conditions. Photoluminescence and electroluminescence spectra of the same compound are shown in Fig. 9. Fig. 9 a) shows the PL spectra under the excitation at 370nm before fabricated, which behaves a low color rendering indices (CRI) of 72 and a high correlated color temperature (CCT) of 5656K with coordinates of (0.3295, 0.3052). While the fabricated w-LED lamp generates a warmer CCT of 2751 K and a superior CRI of 86 with coordinates of (0.3744, 0.3153), the inset displays a photograph of a white-light emission when driven by a 25 mA current. Whereas, EL spectra in Fig. 9 b) shows a distinctive phenomenon that the two emission peaks of $RbBaPO_4$:Eu^{2+} and $NaCaPO_4$:Eu^{2+} fade away by a miracle resulting in the emission intensity of $CsMgPO_4$:Eu^{2+} becoming higher. The PL and PLE spectra of those tri-color

phosphors are shown in **Fig. 10**, and it is found that the excitation peaks for RbBaPO4:Eu^{2+} (near 420nm) and NaCaPO4:Eu^{2+} (near 510nm) phosphors appear lateral overlap with emission peaks of the mixture PL spectra from a range of 400nm to 530nm shown in the dashed area of **Fig. 10**, where $CsMgPO_4$:Eu^{2+} phosphor can absorb the blue and green lights emitted by $RbBaPO_4$:Eu^{2+} and $NaCaPO_4$:Eu^{2+}. This can make clear the mechanism of self-absorption among the mixture between those tri-color phosphors[21], which enhances the long wavelength emissions for *w*-LEDs compared to a blue InGaN LED chip with a yellow phosphor YAG: Ce^{3+}. Therefore, the fabrication experiment of the *w*-LED lamp demonstrate that such phosphors and their mixing strategy are promising for *w*-LEDs.

IV. Conclusions

In summary, blue emission $RbBaPO_4$:Eu^{2+}, green emission $NaCaPO_4$:Eu^{2+} and red emission $CsMgPO_4$:Eu^{2+} phosphors were prepared by a high temperature solid-state reaction method. The emission peaks at near 430 nm, 510nm and 630nm for the obtained samples are ascribed to the 4*f*-5*d* transition of Eu^{2+}. The qualitative analysis between crystal field splitting and coordination number or polyhedron size were employed to explain the observed emission spectra. A white light-emitting diode (LED) lamp was fabricated based on these phosphors combining a 370 nm n-UV chip showing a high color rendering indices (CRI) of 86 and a warm correlated color temperatures (CCT) of 2751K, which indicated that the Eu^{2+}-activated versatile orthophosphate phosphors have the potential application in warm white LEDs.

ACKNOWLEDGMENTS

The present work was supported by the National Natural Science Foundations of China

(Grant No. No.51002146, No.51272242), Natural Science Foundations of Beijing (2132050), the Program for New Century Excellent Talents in University of Ministry of Education of China (NCET-12-0950), Beijing Nova Program (Z131103000413047), Beijing Youth Excellent Talent Program (YETP0635) and the Funds of the State Key Laboratory of New Ceramics and Fine Processing, Tsinghua University (KF201306).

References

1 Z. G. Xia, Y. Y. Zhang, M. S. Molokeev, V. V. Atuchin, Y. Luo, *Sci. Rep.*, 2013, **3**, 3310-3310-7.

2 Z. G. Xia, X. M. Wang, Y. X. Wang, L. B. Liao and X. P. Jing, *Inorg. Chem.*, 2011, **50**, 10134.

3 S. Lee, S. Y. Seo, *J. Electrochem. Soc.*, 2002, **149,** 85−88.

4 C. C. Lin, Y. S. Tang, S. F. Hu, R. S. Liu, *J. Lumin.,* 2009, **129**, 1682-1684.

5 C. L. Zhao, Z. G. Xia and S. X. Yu, *J. Mater. Chem. C,* 2014, DOI: 10.1039/c4tc00488d.

6 Z. P. Yang, G. W. Yang, S. L. Wang, J. Tian, X. N. Li, Q. L. Guo, G. S. Fu, *Mater. Lett.,* 2008, **62**，1884-1886.

7 Y. L. Huang, H. J. Seo, *J. Electrochem. Soc.*, 2011, **158**, 260-263.

8 C. C. Lin, Z. R. Xiao, G. Y. Guo, T. S. Chan, R. S. Liu, *J. Am. Chem. Soc*. 2010, **132,** 3020–3028.

9 L. El Ammari, B. Elouadi, J. *Alloys Compd.*, 1992, **188**, 99-101.

10 M. Ben Amara, M. Vlasse, G. le Flem, P. Hagenmuller, *Acta Crystallogr., Sect. C: Cryst. Struct. Commun.,* 1992, **38,** 127-220.

11 N.Yu. Strutynska, I.V. Zatovsky, V.N. Baumer, N.S. Slobodyanik, *Acta Crystallogr. Sect. E: Struct. Rep*., 2009, **65**, i58-i58.

12 A.C. Larson, R.B. Von Dreele, *Los Alos National Laboratory Report (LAUR)*, 1994, **86**, 748.

13 R. D. Shannon, *Acta Crystallogr.,* 1976, **A32**, 751-767.

14 G.Blasse, B. C. Grabmaier, *Springer Verlag,* Berlin, 1994.

15 L. G. Van Uitert, *J. Lumin.* 1984, **29,** 1.

16 C. Kulshreshtha, A. K. Sharma, K. Sun. Sohn, *J. Electrochem. Soc.*, 2009, **156,** J52-J56.

17 P. Dorenbos, *Phys. Rev. B.,* 2000, **62,** 15650.

18 P. Dorenbos, *Phys. Rev. B.,* **64,** 2001,125.

19 P. Dorenbos, L. Pierron, L. Dinca, C. W. E. van Eijk, A. Kahn-Harari, and B. Viana, *J. Phys. Condens. Matter.* 2003, **15,** 511.

20 M. A. Reshchikov, X. Gu, B. Nemeth, J. Nause, H. Morkoc, *Mater. Res. Soc. Symp. Proc*. 2006, ***892*,** 0892.

21 N. Kaihovirta, A. Asadpoordarvish, A. Sandström, L. Edman, *ACS Photonics*, 2014, **1**, 182–189

The table and figures captions are as follows,

Table 1. Main parameters for $RbBaPO_4:Eu^{2+}$, $NaCaPO_4:Eu^{2+}$, and $CsMgPO_4:Eu^{2+}$ from results of the GSAS Rietveld Refinement

Fig. 1. XRD patterns of $RbBaPO_4:Eu^{2+}$, $NaCaPO_4:Eu^{2+}$ and $CsMgPO_4:Eu^{2+}$ samples, the standard patterns of $RbBaPO_4$ phase (JCPDS-81-647), $NaCaPO_4$ phase (JCPDS-39-1193) and $CsMgPO_4$ phase (JCPDS-45-275).

Fig. 2. Rietveld plots of a) $RbBaPO_4:Eu^{2+}$, b) $NaCaPO_4:Eu^{2+}$ and c) $CsMgPO_4:Eu^{2+}$ samples.

Fig. 3. Photoluminescence excitation (PLE) and photoluminescence (PL) spectrum of blue-emitting $RbBaPO_4$, green-emitting $NaCaPO_4$ and red-emitting $CsMgPO_4$ phosphors.

Fig. 4. a) The normalized emission spectra for $RbBaPO4:Eu^{2+}$, $NaCaPO4:Eu^{2+}$ and $CsMgPO4:Eu^{2+}$ phosphors under the excitation at 340nm. b) Coordination environment of the cations Ba^{2+}, Ca^{2+} and Cs^{+}, respectively.

Fig. 5. Energy diagram of 5d configuration and coordination number of Ba^{2+}, Ca^{2+} and Cs^{+} in $RbBaPO_4:Eu^{2+}$, $NaCaPO_4:Eu^{2+}$ and $CsMgPO_4:Eu^{2+}$ hosts.

Fig. 6. SEM images of the a) $RbBaPO_4:Eu^{2+}$ and b) $NaCaPO_4:Eu^{2+}$ c) $CsMgPO_4:Eu^{2+}$ and d) the mixture of those tri-color phosphors with a wide range of particle size, including agglomerates of the smaller particles.

Fig. 7. The relative intensities of temperature-dependent emission spectra for $RbBaPO_4:0.03Eu^{2+}$, $NaCaPO_4:0.01Eu^{2+}$ and $CsMgPO_4:0.07Eu^{2+}$ samples under the excitation of 340 nm.

Fig. 8. CIE chromaticity diagram and the selected phosphor images of blue-emitting $RbBaPO_4$, green-emitting $NaCaPO_4$ and red-emitting $CsMgPO_4$ orthophosphate

phosphors under 365 nm UV-lamp excitation.

Fig. 9. Photoluminescence and electroluminescence spectra combined with $RbBaPO_4:Eu^{2+}$, $NaCaPO_4:Eu^{2+}$ and $CsMgPO_4:Eu^{2+}$ orthophosphate phosphors: a) PL spectra under the excitation at 370nm. b) EL spectra of *w*-LED lamp fabricated using a 370 nm *n*-UV chip.

Fig. 10. Photoluminescence excitation (PLE) spectrum of blue-emitting $RbBaPO_4$, green-emitting $NaCaPO_4$ and red-emitting $CsMgPO_4$ phosphors and photoluminescence (PL) spectra for the mixture of those tri-color phosphors.

Table 1. Main parameters for $RbBaPO_4:Eu^{2+}$, $NaCaPO_4:Eu^{2+}$, and $CsMgPO_4:Eu^{2+}$ from results of the GSAS Rietveld Refinement

Formula	**$RbBaPO_4:Eu^{2+}$**	**$NaCaPO_4:Eu^{2+}$**	**$CsMgPO_4:Eu^{2+}$**
space group	*Pnma*	*Pn(21)a*	*P1n1*
$\alpha=\beta=\gamma$,°	90	90	90
2θ-interval, °	10-80	10-80	10-80
***a* (Å)**	7.845	20.403	8.930
***b* (Å)**	5.7285	5.400	5.515
***c* (Å)**	10.039	9.158	9.633
***V* (Å^3)**	448.86	1009.16	474.49
Z	4	4	2
R_{wp}(%)	2.67	5.13	5.48
R_p(%)	1.69	3.65	3.97

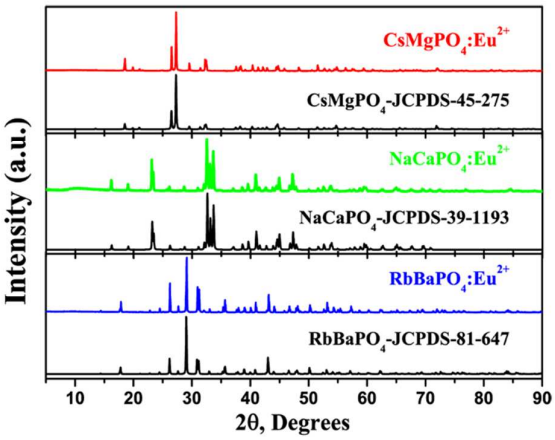

Fig. 1. XRD patterns of $RbBaPO_4:Eu^{2+}$, $NaCaPO_4:Eu^{2+}$ and $CsMgPO_4:Eu^{2+}$ samples, the standard patterns of $RbBaPO_4$ phase (JCPDS-81-647), $NaCaPO_4$ phase (JCPDS-39-1193) and $CsMgPO_4$ phase (JCPDS-45-275).

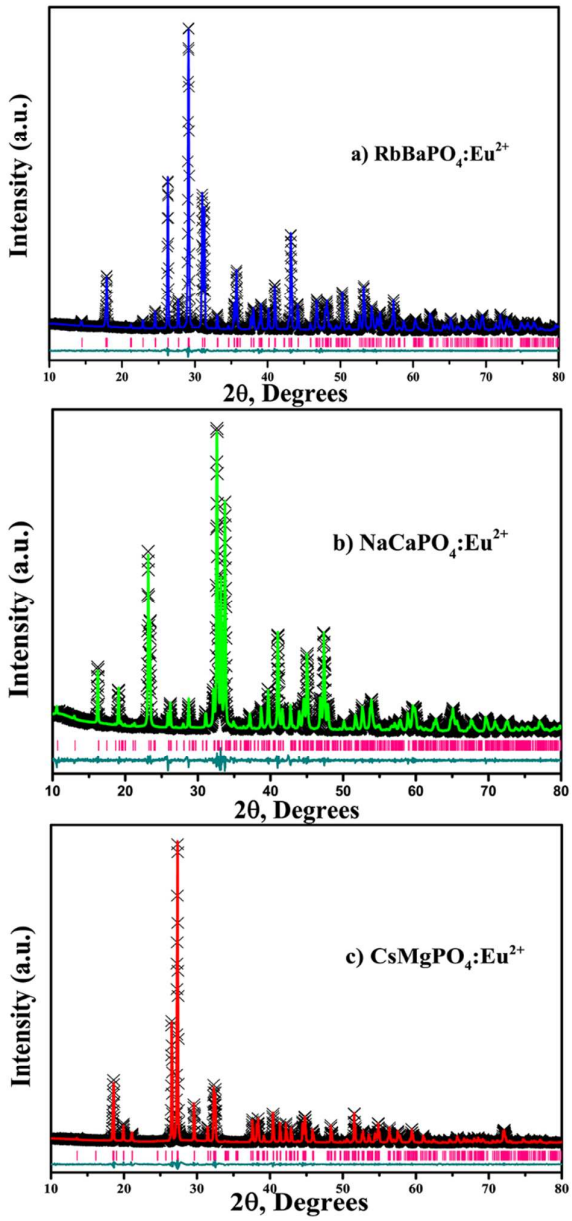

Fig. 2. Rietveld plots of a) $RbBaPO_4:Eu^{2+}$, b) $NaCaPO_4:Eu^{2+}$ and c) $CsMgPO_4:Eu^{2+}$ samples.

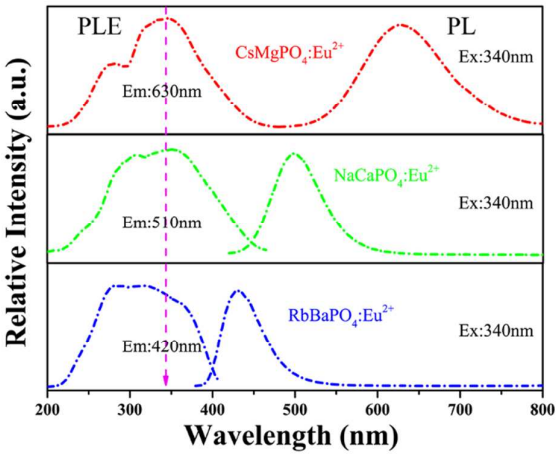

Fig. 3. Photoluminescence excitation (PLE) and photoluminescence (PL) spectrum of blue-emitting $RbBaPO_4$, green-emitting $NaCaPO_4$ and red-emitting $CsMgPO_4$ phosphors.

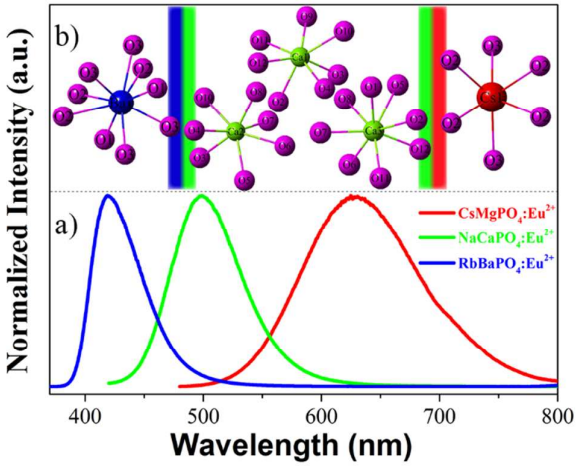

Fig. 4. a) The normalized emission spectra for RbBaPO4:Eu^{2+}, NaCaPO4:Eu^{2+} and CsMgPO4:Eu^{2+} phosphors under the excitation at 340nm. b) Coordination environment of the cations Ba^{2+}, Ca^{2+} and Cs^{+}, respectively.

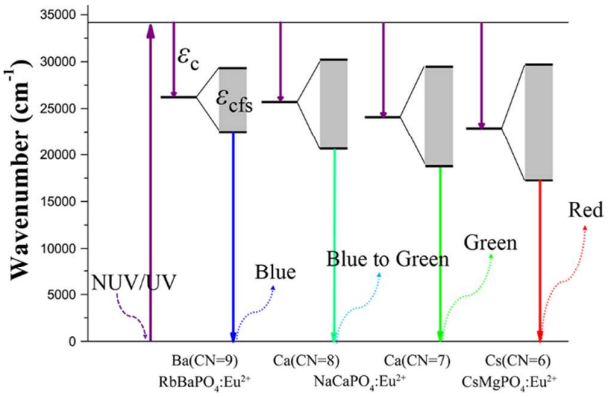

Fig. 5. Energy diagram of 5d configuration and coordination number of Ba^{2+}, Ca^{2+} and Cs^{+} in $RbBaPO_4:Eu^{2+}$, $NaCaPO_4:Eu^{2+}$ and $CsMgPO_4:Eu^{2+}$ hosts.

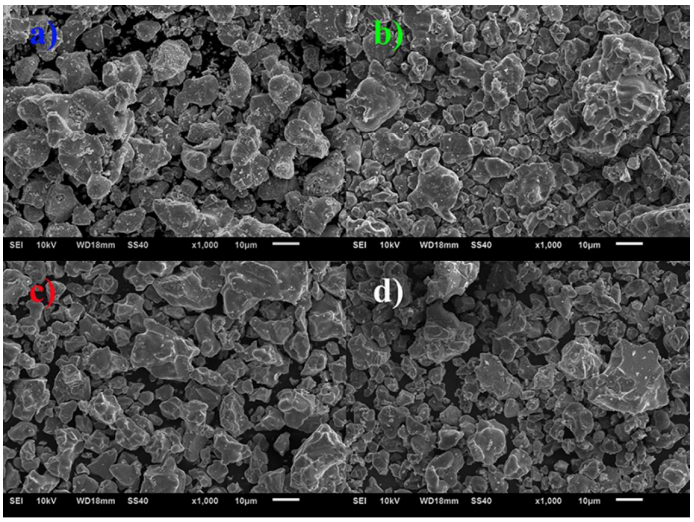

Fig. 6. SEM images of the a) $RbBaPO_4:Eu^{2+}$ and b) $NaCaPO_4:Eu^{2+}$ c) $CsMgPO_4:Eu^{2+}$ and d) the mixture of those tri-color phosphors with a wide range of particle size, including agglomerates of the smaller particles.

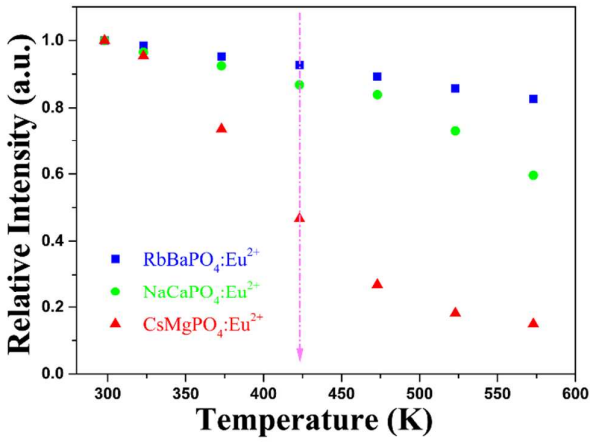

Fig. 7. The relative intensities of temperature-dependent emission spectra for $RbBaPO_4$:0.03Eu^{2+}, $NaCaPO_4$:0.01Eu^{2+} and $CsMgPO_4$:0.07Eu^{2+} samples under the excitation of 340 nm.

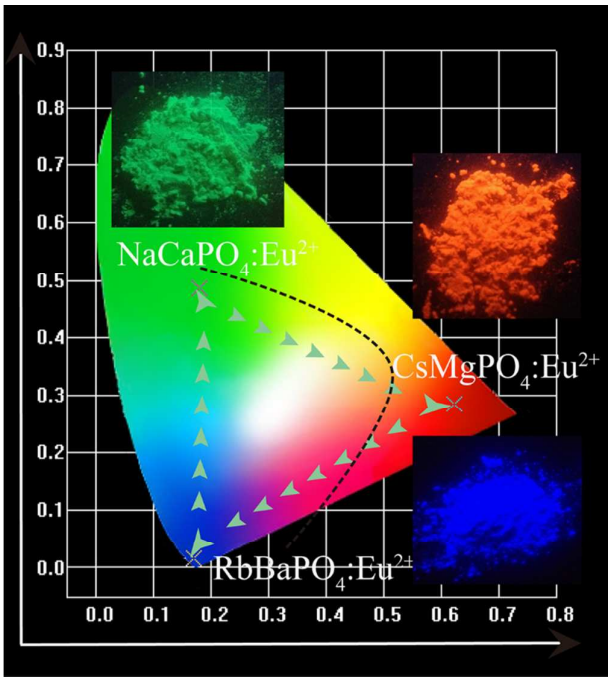

Fig. 8. CIE chromaticity diagram and the selected phosphor images of blue-emitting $RbBaPO_4$, green-emitting $NaCaPO_4$ and red-emitting $CsMgPO_4$ orthophosphate phosphors under 365 nm UV-lamp excitation.

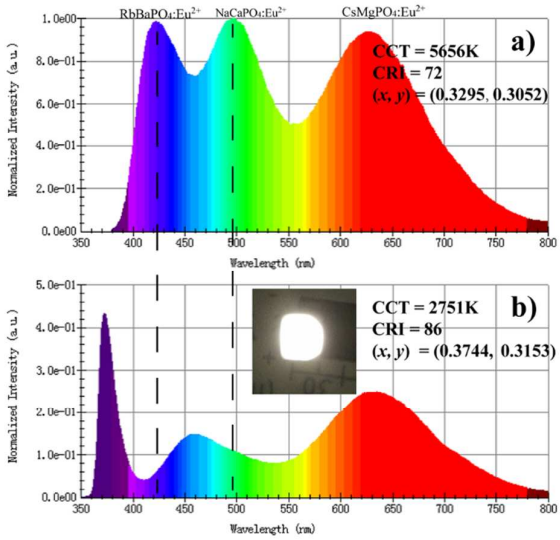

Fig. 9. Photoluminescence and electroluminescence spectra combined with $RbBaPO_4:Eu^{2+}$, $NaCaPO_4:Eu^{2+}$ and $CsMgPO_4:Eu^{2+}$ orthophosphate phosphors: a) PL spectra under the excitation at 370nm. b) EL spectra of *w*-LED lamp fabricated using a 370 nm *n*-UV chip.

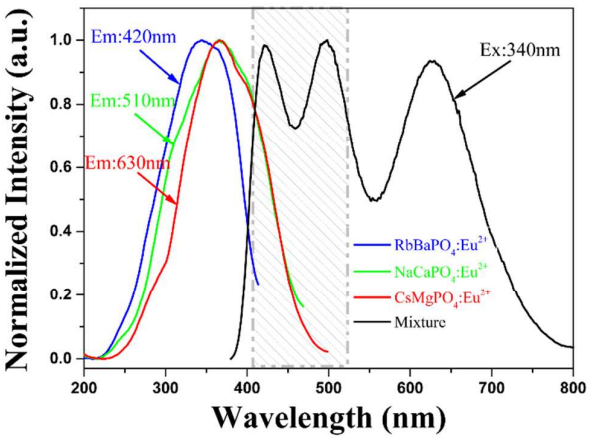

Fig. 10. Photoluminescence excitation (PLE) spectrum of blue-emitting $RbBaPO_4$, green-emitting $NaCaPO_4$ and red-emitting $CsMgPO_4$ phosphors and photoluminescence (PL) spectra for the mixture of those tri-color phosphors.